

CCA-1950

YU ISSN 0011-1643

UDC 541.183

Conference Paper (Invited)

Surface Forces with Adsorbed and Grafted Polymers*

Jacob Klein

Department of Polymer Research
The Weizmann Institute of Science
Rehovot 76100, Israel

Received May 4, 1990

In this lecture we briefly review our understanding of surface forces with adsorbed, neutral flexible polymer chains, and describe some recent studies of surface forces with a range of end-grafted chains. In the latter case we find the polymer layers to be approximately twice the thickness of adsorbed layers of comparable size and surface-excess; we find that the interactions are monotonically repulsive and rate-independent at all surface coverages. Our results are compared with both scaling and mean-field models, and are in very good qualitative and quantitative agreement with both theoretical approaches.

INTRODUCTION

The forces acting between two surfaces in contact or near-contact determine the behaviour of a wide spectrum of physical properties. These include friction, lubrication, the flow properties of particulate dispersions, and, in particular, the stability of colloidal systems.¹⁻³ In the latter, which include both biocolloids and man-made dispersions, the interactions between the particles as they approach determine whether they remain dispersed or whether they will stick together (for example, under van der Waals attraction) and sediment.¹⁻³ Colloidal stability can be achieved in ionic (such as aqueous) media when the particles have a surface charge (leading to double-layer repulsion, which is well described by DLVO⁴ theory); but the use of polymeric chains which attach to the surface of the particles is becoming increasingly common in the stabilising of such dispersions, and is effective in both ionic and non-ionic media.⁵ The reason for the efficacy of polymers in such stabilisation is because their large size results in thick adsorbed layers, which may repel each other and effectively prevent approach of the underlying surfaces to a separation where van der Waals attraction between the particle surfaces leads to their adhesion. At the same time, the length and flexibility of polymeric chains frequently allows them to adsorb strongly

* Based on an invited lecture presented at the 8th »Ruđer Bošković« Institute's International Summer Conference on the Chemistry of Solid/Liquid Interfaces Red Island, Rovinj, Croatia, Yugoslavia, June 22 — July 1, 1989.

and irreversibly (while still extending a long way from the surface) due to the large number of adsorbing sites on any one chain. This combination of weak adhesion energy per site (which results in thick layers) and the large *overall* sticking energy per chain - which ensures strong adsorption - is the crucial characteristic of adsorbed flexible chain.

The use polymers as colloidal stabilisers has a long history, going back to the empirical development by the ancient Egyptians, who would stabilise carbon-black dispersed in water by adding trace amounts of a soluble polysaccharide (gum arabic, the resin of the acacia tree), to form a long-enduring ink. Nowadays, at a different level of sophistication, vast quantities of colloidal dispersions in paints, emulsions, foams, pharmaceuticals and ferrofluids are stabilised by attaching polymers to the particulate surfaces.⁵ Interactions between surfaces bearing attached polymer chains are primarily determined by the interactions between the segments, which can be repulsive (in a good solvent) or attractive (in a poor solvent, (Figure 1(a)).⁶⁻⁸ Such forces (between surfaces bearing *adsorbed* polymers) have been studied directly and extensively over the past decade, using the mica approach.⁹ These studies demonstrated not only the importance of the solvent quality, but also the great importance of so-called 'bridging attraction' between two surfaces. Such bridging takes place whenever a given chain spans the intersurface gap, adsorbing quasi-irreversibly on both surfaces (Figure 1(b)). Bridging attraction dominates the surface interactions especially at low adsorbances,⁷ even for the case of good solvents where at high adsorbance there is a net repulsion;¹⁰ such attraction is highly undesirable *en route* to a stabilised dispersion, but can be overcome by using chains which *do not adsorb*, and hence cannot bridge, but which are attached at one end to the surface by a chemical or physical bond (Figure 1(c)).

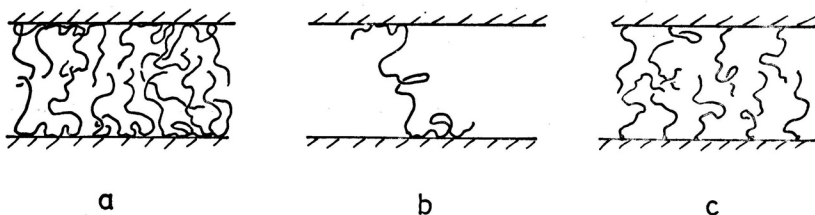


Figure 1. Illustrating interactions between surfaces bearing (a) adsorbed; (b) bridging and (c) grafted polymers.

Together with my colleagues H. J. Taunton, C. Toprakcioglu and L. J. Fetters, we recently completed a study of the forces between two surfaces bearing nonadsorbing polymers attached at one end only. This review lecture will briefly consider our understanding of forces with *adsorbed* chains, and will then go on to describe some of these more recent results with the end-anchored polymers; we shall then discuss them in the context of recent theoretical models of such interactions.

SURFACE FORCES WITH ADSORBED POLYMERS

The mica force-measurement technique, pioneered in Cambridge by Winterton and Tabor¹ in 1968 and Israelachvili and Tabor,¹² in 1971, and subsequently greatly extended by Israelachvili and co-workers, especially to the case of liquid media,¹³ enables the forces between two atomically smooth surfaces of mica a closest distance D apart to be accurately measured. The range of D accessible is typically some thousands of Angstroms, and is measured using multiple beam interferometry with a resolution around $\pm 2 \text{ \AA}$. The two surface are mounted opposite each other in a crossed cylinder configuration, and the force $F(D)$ between them is determined by observing the deflection of a leaf spring on which the lower surface is mounted in response to an externally applied displacement of the top, rigidly mounted surface. A schematic illustration of the apparatus, built and used at the Weizmann Institute¹⁴ to determine $F(D)$ between polymer-bearing surfaces, is shown in Figure 2. Over the past decade the interactions between mica surfaces with adsorbed chains in a variety of conditions have been characteri-

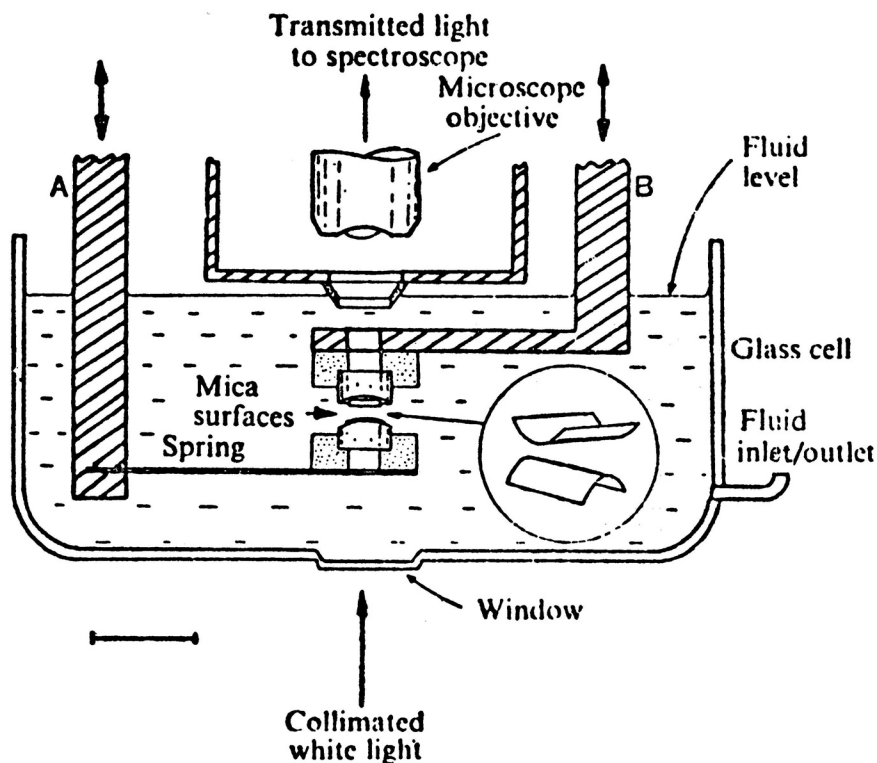


Figure 2. Schematic section of the force-measurement apparatus used at the Weizmann Institute. The mica surfaces are half-silvered to allow white-light interference fringes to form, and are mounted in a crossed-cylinder configuration (inset) to avoid alignment problems. As the top surface is moved *via* its rigid support, the inter-surface force deflects the spring on which the lower surface is mounted, to give the forces directly. The scale bar is 3 cm.

sed using the mica approach, and these are schematically summarised¹⁵ in Figure 3. We note in particular that at low adsorbed amounts (broken curves in Figure 3) the initial interaction on approach of the polymer bearing surfaces is always *attractive*, due to bridging effects as noted earlier. The nature of these forces is reasonably well understood in terms of molecular models, and has been described in detail in recent reviews.²²

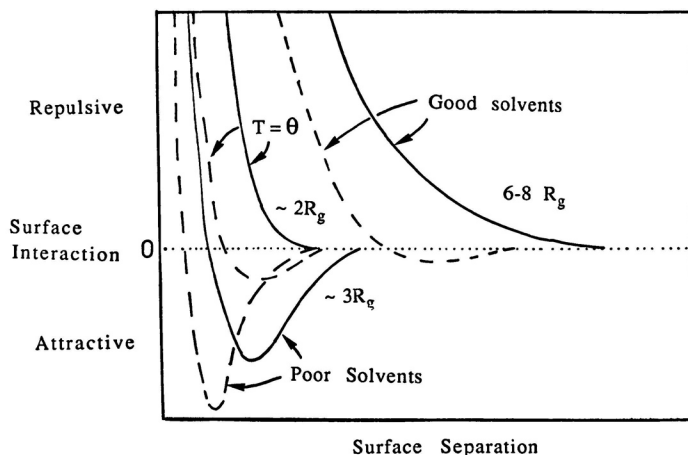


Figure 3. Summary of interaction-energy *vs.* surface separation laws for surfaces with adsorbed chains. The solid curves are for high surface coverage, with the broken curves showing the corresponding behaviour with low surface-coverage.

In the course of our studies on interactions between mica surfaces in polymer solutions, we discovered that the model polymer polystyrene (PS) would not adsorb onto mica from the good solvent toluene.⁸ This polymer thus serves well for studies of grafted chains on mica: by functionalising one of its ends so that the polymer attaches to the mica surfaces, we deduce unambiguously that we must have a system such as illustrated in Figure 1(c), as the only binding site is known to be at the end of the chain.

TABLE I
Molecular characteristics of PS-X synthesised as in ref. 17

Sample	M_w	M_w/M_n	R_o (Å)	R_F (Å)
PS-X(26k)	26,500	1.02	112	122
PS-X(58k)	58,000	1.10	169	197
PS-X(140k)	140,000	1.03	258	323
PS-X(375k)	375,000	1.03	422	575
PS-X(660k)	660,000	1.02	559	801

TABLE II
Molecular characteristics of PS-PEO
(Obtained from and characterized by Polymer Laboratories, U.K.)

Sample	M_w	M_w/M_n	PEO content, %	(PS) _x (PEO) _y wt. av. D. P.		R_F (Å)
				x	y	
PS-PEO(150k)	150,000	1.16	1.5	1420	51	340
PS-PEO(184k)	184,000	1.10	4	1700	167	393

R_0 and R_F are the unperturbed dimensions and swollen Flory radius respectively.

SURFACE FORCES WITH GRAFTED CHAINS^{16,17}

A series of polystyrene chains was synthesised anionically,¹⁷ covering a range of molecular weights and terminated with the zwitterionic group —(CH₂)₃ N⁺(CH₃)₂(CH₂)₃ SO₃⁻, henceforth referred to as -X; their molecular characteristics are shown in Table I. Two samples of PS terminated with short polyethylene oxide (PEO) moieties were also used, Table II; PEO is known to adsorb strongly to mica from toluene,⁸ and these PS-PEO diblocks are end-anchored to the mica *via* the PEO tail, which thus serves the same purpose as the zwitterionic group -X. A non-functionalised PS sample was also synthesised, and used as a control. In a typical experiment the mica sheets are mounted opposite each other (Figure 2) and the optical interference between them determined at contact in air. Solvent is then added

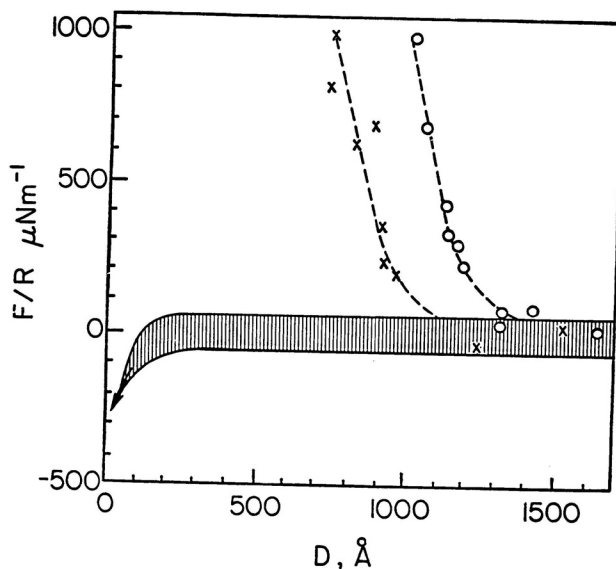


Figure 4. Force-distance profile between two curved mica surfaces (radius R) immersed in a solution (ca. 10^{-4} w/w) of PS-PEO (150k) in toluene, and held at a surface separation of ca. $40 \mu\text{m}$. The crosses are for a profile measured after 30 minutes incubation, while the circles show the force measured 12 hours later (equilibrium coverage). The shaded band covers the scatter of the force profile in polymer-free solvent and in a solution of unfunctionalised PS.

and the force-distance profile $F(D)$ of the interactions between the surfaces -- when they are a distance D apart -- is measured. Unfunctionalised polystyrene is added to the cell and $F(D)$ is again measured after allowing for overnight equilibration. This stage is essential as a control to verify that in the *absence* of the zwitterionic group, no adsorption occurs. Finally, the PS-X (or PS-PEO) sample is added to the solution, and $F(D)$ determined at increasing times. Results of such an experiments for sample PS-PEO (150K), and for sample PS-X(140K), of molecular weight 140,000, are shown in Figure 4 and 5. The schematic interpretation of each of the three stages is shown in Figure 6.

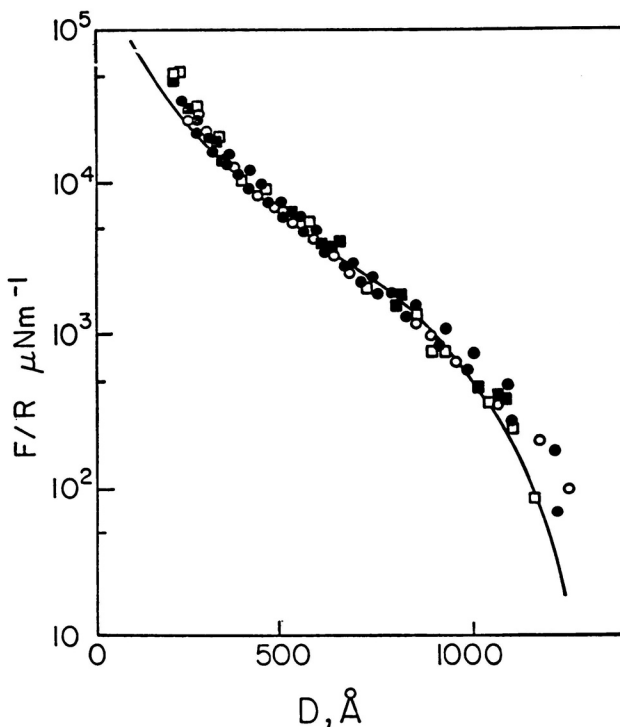


Figure 5. Force-distance profiles between curved mica sheets following incubation to saturation in a solution (ca. 10^{-4} w/w) of PS-X (140k) in toluene. Different rates of compression and decompression were used, and results are shown for two different experiments. The solid line corresponds to the prediction of the Alexander-de Gennes model, based on equation (2).

We note a number of features here which were characteristic of all force distance profiles with grafted chains of the PS-X or PS-PEO type. As shown in Figure 4, the $F(D)$ profile following 30-minutes incubation was already long-ranged and repulsive, reaching its limiting value after some hours. This suggests a rapid initial stage of attachment of polymer by its adhering (-PEO or -X) end to the surface; our attempts to detect bridging attraction at short incubation times -- as was done with adsorbing chains in good solvents

— were uniformly unsuccessful due to this rapid appearance of a long-ranged repulsion. We also note — Figure 5 — that the rates of compression and decompression of the surfaces made little difference, within the scatter, to the form of $F(D)$. This is in contrast to the relaxations observed with adsorbed chains in good solvents⁸ and is probably due to the fact that — for the latter case — strong compression had the effect of forcing additional monomers onto the surface with a consequent relaxation time for these to desorb again to the equilibrium structure. For the case of the non-adsorbing PS-X or PS-PEO chains — which are attached to the surface at one end only — such an effect (which results in different $F(D)$ profiles at rapid and at slow decompression rates) is expected to be absent, as is indeed observed, Figure 5.

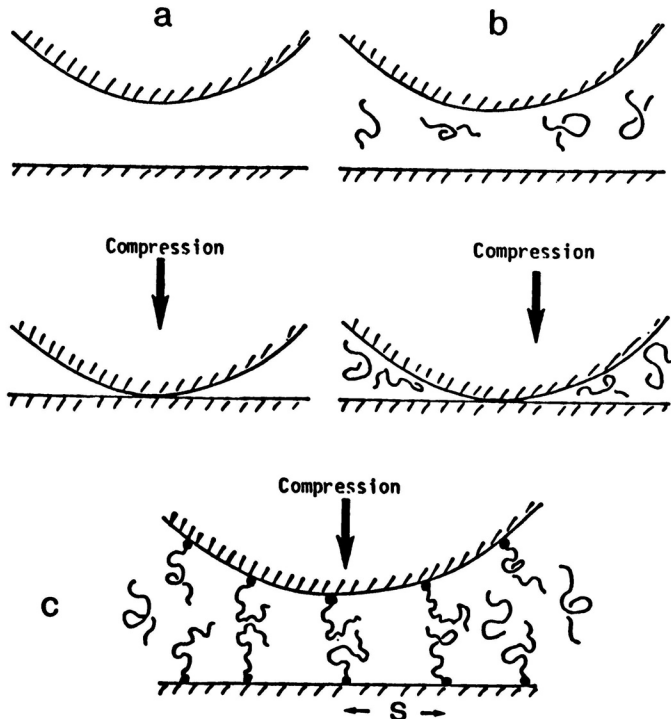


Figure 6. Schematically showing the three stages of interactions:

- (a) in polymer-free solvent
- (b) following addition of unfunctionalised, hence non-adsorbing, polystyrene. Interaction profiles for both (a) and (b) correspond to the shaded band in Figure 4.
- (c) Following addition of PS-X or PS-PEO and its attachment to the surface. The interaction profiles in this case correspond to these shown by the data points in Figures 4 and 5.

The shape of the force profile and its variation with intersurface separation D will be considered in greater detail later. We note here that for all the PS-X samples, (as well as for the two polystyrene-poly(ethylene oxide) diblock copolymers) the qualitative variation of $F(D)$ with D was similar,

once account is taken of the different range for onset of interaction, $2L_{\text{onset}}$. Thus, from Figure 5, $2L_{\text{onset}}$ for PS-X(140) is estimated as $1350 \pm 100 \text{ \AA}$, and onset values $2L_{\text{onset}}$ for the other PS-X samples were similarly estimated from their respective $F(D)$ profiles.¹⁷ These are tabulated in Table III.

TABLE III
Mean surface separations $2L_{\text{onset}}$ at onset of detected repulsion

Sample	$2L_{\text{onset}}$ (Å)
PS-X(26k)	440 ± 50
PS-X(58k)	800 ± 80
PS-X(140k)	1350 ± 100
PS-X(375k)	2400 ± 100
PS-X(660k)	2100 ± 100
PS-PEO(150k)	1450 ± 100
PS-PEO(184k)	1500 ± 100

We note in particular that range of the interactions, and thus the layer thickness of the end-anchored chains, is around 6–8 R_g , where R_g is the corresponding unperturbed radius of gyration, for the chains. In absolute terms these values imply that — for the polymer surface excess values in our studies, which are comparable to the adsorbance of *adsorbing* chains in good solvents⁸ — the layers are roughly twice the thickness of the adsorbed layers for a given chain size. In Figure 7 we show $F(D)$ profiles for all the PS-X samples studied (and also for two PS-PEO samples, which behave in a very similar fashion), on a master plot where the surface separation (D) axes for the different molecular weights have been scaled by the repulsion onset separation $2L_{\text{onset}}$. In obtaining the master plot the respective force-axes have, in addition, been multiplied by different factors for the different $F(D)$ profiles. These multiplication factors depend on the molecular weight of the PS-X chains, and are related to the adsorbed amount of each chain.¹⁷ We note from Figure 7 in particular that the force-distance interaction profiles with end-grafted polymer, once the $2L_{\text{onset}}$ scaling has been carried out, fall closely on a single curve. This feature is considered in the following section in the context of current theoretical models.

Finally, in these experiments we determined¹⁷ the refractive-index *vs.* surface separation profile, which permits the evaluation of the surface excess of polymer.¹⁴ This was done in detail for the case of PS-X (140K); from the amount per unit area (and hence the chain surface density), it was possible to estimate the mean spacing between anchor points, as $s = 85 \pm 10 \text{ \AA}$ for this polymer.¹⁷

MODELS OF END-GRAFTED POLYMER CHAINS

An early model of the structure of end-grafted polymer chains, each of N monomers and with a mean interanchor spacing s (Figure 8(a)) (for $s \ll R_F$, the swollen or Flory radius) was presented by S. Alexander¹⁸ in 1977. According to this, two main factors influence the layer thickness of the grafted layer in a good solvent medium. On the one hand, segments on different (adjacent) chains tend to repel each other, and thus to stretch the

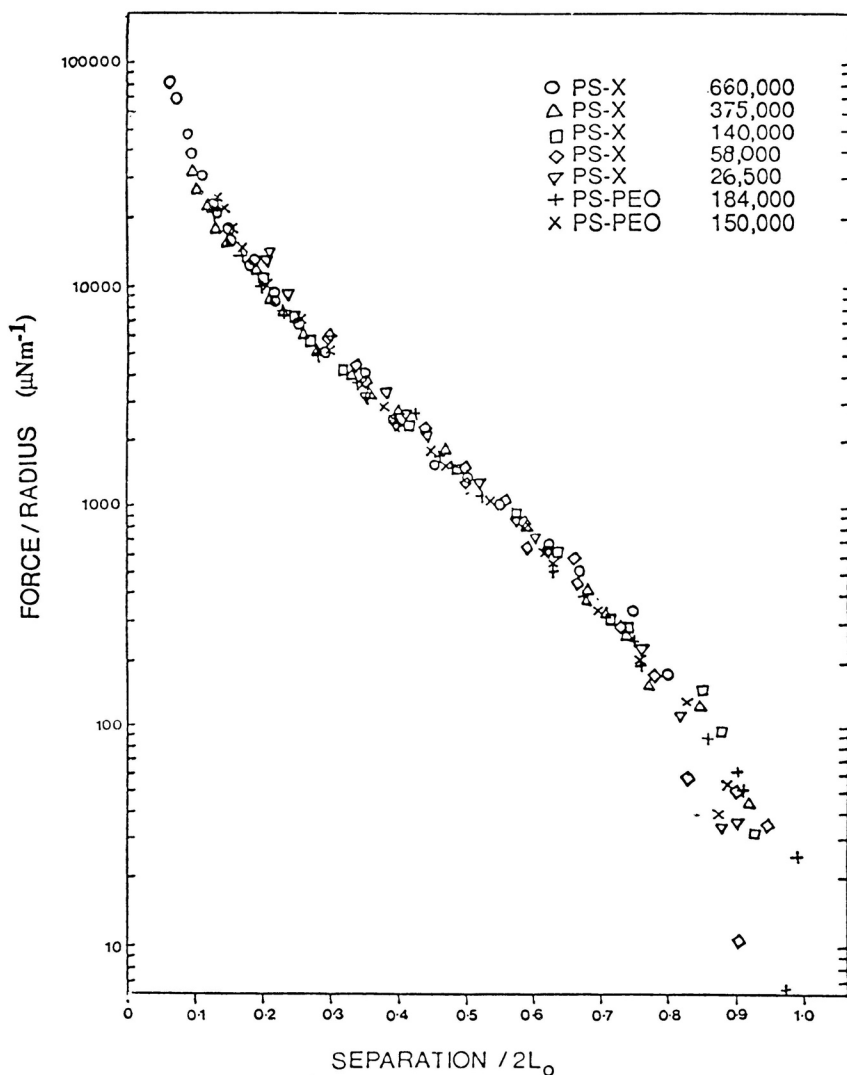


Figure 7. Master curve of force profiles incorporating data from all PS-X and PS-PEO samples. One or two compression-decompressions are shown for each polymer. The horizontal axis has been scaled by the separation $2L_{\text{onset}}$ (Table III) at which forces were first measured.

chains, reduce the overall segment density within the grafted layer and reduce the osmotic free energy. On the other hand, chains resist being stretched beyond their equilibrium configurations (typically of size R_F in a good solvent). By minimising the total free energy associated with two effects, Alexander predicted¹⁸ an equilibrium layer thickness L_0 , scaling as

$$L_o = \text{const. } s (R_F/s)^{5/3} \quad (1)$$

$$= \text{const. } Ns^{-2/3} a^{5/3} \quad (1a)$$

where the swollen Flory radius is given by $R_F = N^{3/5} a$, a being a monomer size.

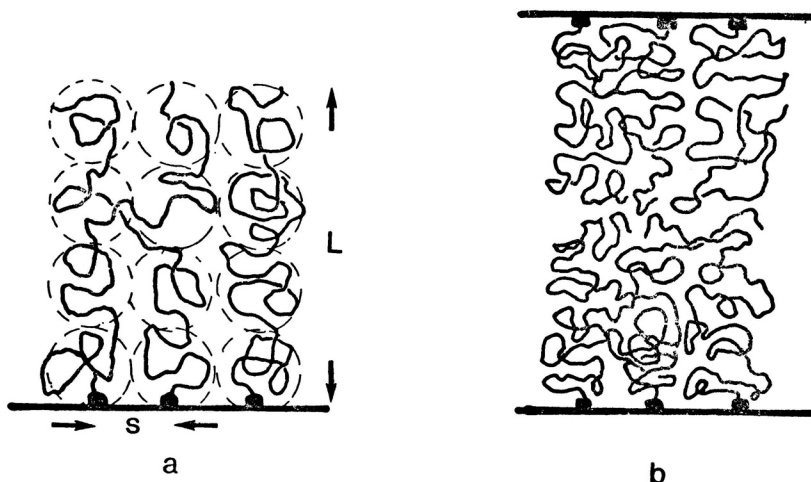


Figure 8. (a) Illustrating the Alexander picture of end-grafted chains as a array of close packed blobs.

(b) Illustrating de Gennes' hypothesis of no interpenetration on compression of the grafted layers.

The Alexander model assumed that the segment density distribution within the layer thickness L_o was uniform, and used a scaling approach¹⁹ (*i. e.* treated chains as consisting of connected correlation zones, or 'blobs', within which excluded volume effects applied, but which were screened from each other) to obtain the relation (1). Scaling approaches cannot yield precise prefactors,¹⁹ hence the unknown constant (of order unity) in equation (1).

The Alexander approach was subsequently extended by de Gennes, to the case of the interaction between two plates bearing grafted chains.²⁰ Using the Alexander model, with the additional assumption that as the grafted layers are compressed against each other they do not interdigitate (Figure 8(b)), the following expression for the force $f(D)$ per unit area between such plates a distance D apart was derived:

$$f(D) = \frac{\text{const. } k_B T}{s^3} [(2L_o/D)^{9/4} - (D/2L_o)^{3/4}], \quad D < 2L_o \quad (2)$$

where k_B and T are Boltzmann's constant and the temperature respectively.

The two terms represent, on the one hand, the increase in free energy due to increased osmotic repulsion as the gap D between the surfaces decreases; and on the other hand, the reduction in free energy at decreasing D as the grafted chains are compressed from their 'over-extended' length L , closer

to equilibrium. Once again, the result is obtained within an unknown constant prefactor of order unity.

Quite recently this simple (though appealing) Alexander-de Gennes picture has been augmented by a number of different approaches, using more sophisticated calculations and not involving the use of assumption such as a uniform segment density and non-interdigitating opposing layers. The most detailed of these is the model by Milner, Witten and Cates,²¹ who use a mean field approach to evaluate the structure of the grafted layers and also interactions between two surfaces bearing such layers. While the Milner-Witten-Cates calculations provide a much more detailed picture of the grafted layer (predicting, for example, a parabolic²¹ rather than a uniform density profile for the monomers in the layer), their predictions of the force-distance profiles are qualitatively and also quantitatively similar to the scaling approach. For this reason we shall find it more convenient in the context of this lecture to discuss our results in terms of the relation of equation (3).

Our results (*e.g.* Figures 5 and 7) are plotted in terms of the actual measured force $F(D)$ divided by the mean radius of curvature R of the mica sheets. This quantity $F(D)/R$ is directly related (*via* the Derjaguin approximation¹³) to the mean interaction energy $E(D)$ between two flat parallel surfaces a distance D apart obeying the same force law. The value of $E(D)$ according to the Alexander-de Gennes model is obtainable by integrating¹⁶ the theoretical force-law of equn. (2), and thus we can directly compare equn. (2) with our measured values of $F(D)/R$.

When this is done for the case of PS-X (140 K), we obtain the fit shown as a solid line Figure 5. The value of s in equn. (2) was taken as 85 Å, as determined from the refractive index data. Two comments concerning this fit should be made: the value of L_o was taken as $L_o = L_{\text{onset}} = 650$ Å, *i.e.* half the separation for onset of interaction — as indicated by the experimental curve at the point where monotonic repulsion is first observed above the scatter. Secondly, the value of the constant prefactor (which cannot be predicted by a scaling approach) used in equation (2) to obtain the solid line shown in Figure 5 was 1.5, consistent with the values of order unity expected in such models. We also note that, from equation (1), setting the constant prefactor (undetermined within order unity) equal to 1, we may calculate (using the known values of R_F and the experimentally evaluated $s = 85$ Å) $L_c = 740 \pm 50$ Å, compared with the experimentally indicated value (as also used for the fit of Figure 5) of 650 ± 50 Å. Once again, the scaling predictions are *quantitatively* close to the scaling prediction. It is appropriate to note that the mean-field calculations of Milner *et al.*^{21(b)} also give a good description (with no need for any adjustable parameters) of both L_o and the $F(D)$ profile for PS-X (140 K).

Finally it is of interest to examine the validity of relation (1b), predicted by both the scaling¹⁸ and the mean-field approaches.²¹ We recall that what is kept constant in our experiments (at least for the series of PS-X chains) is the *adhesion energy* between the end-anchored chains and the mica surfaces, due to the fact that — for all chain lengths — the zwitterionic, anchoring end-group is the same. It is then straightforward to show¹⁷ that the mean interanchor spacing s should *increase* with chain size, if the repulsive ener-

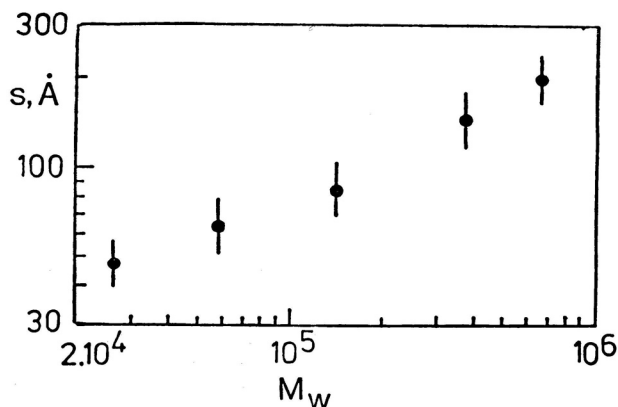


Figure 9. Double logarithmic plot of mean interanchor spacing s of PS-X(M) on the mica surfaces, as a function of M , estimated as described in the text.¹⁷

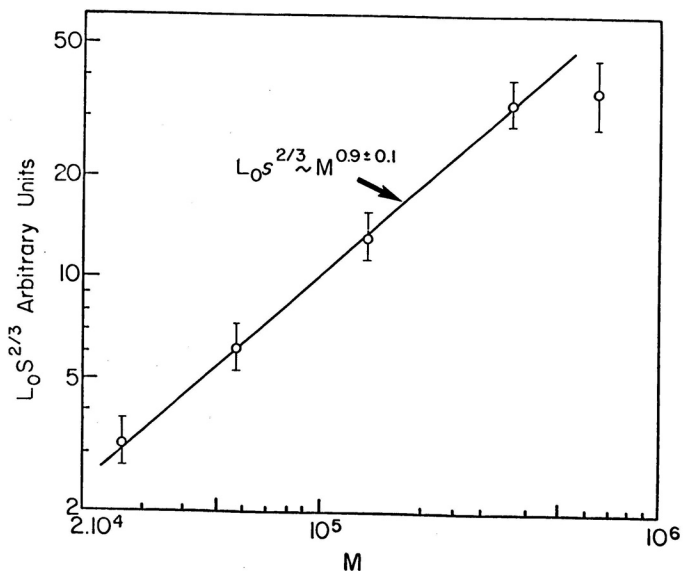


Figure 10. Double logarithmic plot of the variation of $L_0 s^{2/3}$ (arbitrary units) with M for PS-X(M) (see equn. 1(b)).

gies associated with anchoring a chain to the surface are to be balanced against the sticking energy of the zwitterion-mica contact. We obtain a measure of how s changes, with PS-X molecular weight, by examining the highly repulsive regime at small separations D of the profiles for each PS-X sample. At these high compressions the repulsion may be related to the osmotic interactions¹⁹ due to the mean monomer concentrations in the gap, and thus the relative surface excess of the polymers may be estimated.¹⁷ These in turn permit an estimate¹⁷ of the relative s values, and we plot these against the

molecular weights M of the PS-X samples, in Figure 9, where we use the value of s directly determined for PS-X (140 K) to establish the absolute s scale. We see that s does indeed increase with M , as expected. Finally, using the values of L_{onset} (Table II) and s (determined as indicated above), and taking $L_o = L_{\text{onset}}$, we may plot $L_o s^{2/3}$ against M , as suggested by equn. 1(b) and by the mean-field models. This is done in Figure 10. A power-law relation is indeed obtained, showing

$$L_o s^{2/3} = \text{const. } N^\beta$$

where $\beta = 0.9 \pm 0.1$, close to the theoretically predicted value $\beta = 1$.

We may summarise this lecture as follow:

1. End-anchored chains form thick surface layers on a solid surface in good solvent conditions: the layer thickness is typically twice that of *adsorbed* polymer layers for comparable surface-excess values and polymer molecular weights.

2. The interaction between two surfaces bearing end-anchored chains in these good solvent conditions is monotonically repulsive, shows no hysteresis or relaxation effects at rapid compression-decompression rates, and no evidence of any bridging attraction even at low adsorbed amounts. These features are markedly different to those characterising interactions between surface with *adsorbed* chains, where bridging attraction and long-time relaxation effects are prominent.

3. The variation of the force-distance profile is in good quantitative accord with both scaling and mean field models, over several orders of magnitude in the force. In particular, the scaling of the layer thickness with chain length, when due account is taken of the polymer grafting density on the surface, is in good accord with both types of model.

Acknowledgements. — The force-profiles summarised for adsorbed chains were measured with my co-workers P. F. Luckham and Y. Almog, while the work on the end-anchored chains described in this review lecture was carried out together with my co-workers Hillary J. Taunton, Chris Toprakcioglu, and Lewis J. Fetters. A more detailed account of this latter work will shortly appear. I am especially grateful to Professor Velimir Pravdić and other members of the organising committee of the Ruđer Bošković Summer Conference for inviting me to a magnificent venue, and to a most enjoyable and fruitful meeting.

REFERENCES

1. For a recent review see J. W. Goowin (Ed.), *Colloid Dispersions*, Royal Society of Chemistry Special Publication No. 43, Royal Society of Chemistry, London 1982.
2. See for example *Polymer Adsorption and Dispersion Stability*, E. D. Goddard and B. Vincent (Eds.), *American Chemical Society Symposium Series* **240** (1984) 227.
3. D. H. Napper, *Polymeric Stabilisation of Colloidal Dispersions*, Academic Press, London 1983.
4. E. G. W. Verwey and J. Th. G. Overbeek, *Theory of the Stability of Lyophobic Colloids*, Elsevier, Amsterdam, 1948.
5. B. Vincent, *Adv. Colloid Interface Science* **4** (1974) 193.
6. J. Klein, *Nature* **228** (1980) 248.
7. Y. Almog and J. Klein, *J. Colloid Interface Sci.* **106** (1985) 23.

8. J. Klein and P. F. Luckham, *Macromolecules* **17** (1984) 1041.
P. F. Luckham and J. Klein, *Macromolecules* **18** (1985) 721.
9. J. Klein, in: *Molecular Conformations and Dynamics of Macromolecules in Condensed Systems*, M. Nagasawa (Ed.), Elsevier, (Holland) 1988, p. 333.
10. J. Klein and P. F. Luckham, *Nature* **308** (1984) 836.
11. D. Tabor and R. H. S. Winterton, *Proc Roy. Soc. (London)* **A312** (1969) 435.
12. J. Israelachvili and D. Tabor, *Proc. Roy. Soc. (London)* **A331** (1972) 19.
13. J. N. Israelachvili and G. Adams, *J. Chem. Soc. Faraday I* **79** (1978) 975.
14. J. Klein, *J. Chem. Soc. Faraday I* **79** (1983) 99.
15. J. Klein, *Physics World* (June 1989), p. 37.
16. H. J. Taunton, C. Toprakcioglu, L. J. Fetters, and J. Klein, *Nature* **332** (1988) 712.
17. H. J. Taunton, C. Toprakcioglu, L. J. Fetters, and J. Klein, *Macromolecules*, in press.
18. S. Alexander, *J. de Physique (Paris)* **38** (1977) 983.
19. P. G. de Gennes, *Scaling Concepts in Polymer Physics*, Cornell University Press, Ithaca, N. Y. 1979.
20. P. G. de Gennes, *C. R. Hebd Seances Sci.* **300** (1985) 839.
21. a. S. Milner, T. Witten, and M. Cates, *Macromolecules* **21** (1988) 2610.
b. S. Milner, *Europhysics Letters* **7** (1988) 695.
22. P. G. de Gennes, *Adv. Colloid Interface Sci.* **27** (1987) 189.

SAŽETAK

Površnske sile u adsorbiranim i nakalemljenim polimerima

J. Klein

Pregledno su opisane teorije i eksperimentalni rezultati mjerenja površinskih sila s adsorbiranim, neutralnim i fleksibilnim polimernim lancima polistirena, posebno onih s nakalemljenim funkcionalnim skupinama na kraju lanca. Uloga polimera u proučavanju procesa koagulacije odnosno stabilizacije nalazi se u slabim adhezijskim energijama po površinskom mjestu (što dovodi do debelih slojeva), ali i visokoj ukupnoj energiji prijanjanja po lancu (zbog dužine i fleksibilnosti lanca). Za polimere s nakalemljenim funkcionalnim skupinama *zwitterionskog* tipa, ili poli-etilenoksidom pokazano je da su adsorbirani slojevi dvostruko deblji nego u slučaju neutralnog polistirena, te da su interakcije monotono odbojne i neovisne od brzine perturbacije (kompresije ili ekspanzije sloja), bez efekata histereze ili relaksacije. Varijacija odnosa sile prema udaljenosti od površine dobivena mjerenjima na aparatu s tinjčevim površinama, u dobrom je skladu s postojećim teorijama.